Correlation of test results and influence of a mass balance constraint on risks in conformity assessment of a substance or material

(Article begins on next page)

06 October 2024

Measurement

Correlation of test results and influence of a mass balance constraint on risks in conformity assessment of a substance or material

--Manuscript Draft--

Manuscript Number:	
Article Type:	Research Paper
Keywords:	Conformity assessment; Mass balance constraint; Compositional data; Bayesian multivariate modelling; Monte Carlo method; Risk of false decisions
Corresponding Author:	Ilya Kuselman, D.Sc. Independent Consultant on Metrology Modiin, ISRAEL
First Author:	Ilya Kuselman, D.Sc.
Order of Authors:	Ilya Kuselman, D.Sc.
	Francesca R. Pennecchi
	Aglaia Di Rocco
	D. Brynn Hibbert
	Michela Sega
Abstract:	When components of a substance or material are subject to a mass balance constraint, test results of the components' contents are intrinsically correlated because of the constraint. That is in addition to possible metrologically-related correlation of test results, and natural and/or technological correlation of the components' contents. Such correlations may influence understanding of compositional data and evaluation of risks in conformity assessment of the substance or material due to measurement uncertainty. A Bayesian multivariate approach to evaluate the conformance probability of multicomponent materials or objects and corresponding risks of false decisions, able to take into account all observed correlations including spurious, is discussed for different scenarios of compositional data. A Monte Carlo method, which includes the mass balance constraint, written in the R programming environment is provided for the necessary calculations. A technique for separation of spurious correlations from experimental (natural and/or technological) correlations is proposed.

Cover letter

Professor Paolo Carbone,

Editor-in Chief, Measurement   09 April, 2020

Dear Prof. Carbone,

Please find attached the manuscript by Francesca R. Pennecchi, Aglaia Di Rocco, Ilya Kuselman, D. Brynn Hibbert and Michela Sega, titled "Correlation of test results and influence of a mass balance constraint on risks in conformity assessment of a substance or material", which we would like to publish in Measurement.

Novelty Statement:

Three models of prior and likelihood describing composition of a multicomponent material or substance, which consider requirements of a mass balance and different kinds of correlation among the components' contents, are proposed in the framework of a Bayesian multivariate approach.

   A Monte Carlo method, coded in the R programming environment, is reported for calculations of the prior coverage probability and the total global risks of false decisions on conformity of the material or substance, taking into account the mass balance constraint.

Declaration of interest: There is no any actual or potential conflict of interest of any author.

Submission declaration and verification: The work described has not been published previously, it is not also under consideration for publication elsewhere. The publication in Measurement is approved by all the authors.

The manuscript was previously submitted to Talanta (on 08.03.20) and rejected on due to outside the scope of the journal: the editor, Dr. Joaquim Nobrega, has recommended to submit it to a metrological journal.

Best regards,

Dr. Ilya Kuselman,
the manuscript corresponding author,
ilya.kuselman@gmail.com

ilya.kuselman@bezeqint.net

HIGHLIGHTS

- Three kinds of correlation of component contents involved in a mass balance are discussed
- Three Bayesian multivariate models describing compositional data are proposed
- A Monte Carlo method for conformity assessment at a mass balance constraint is developed
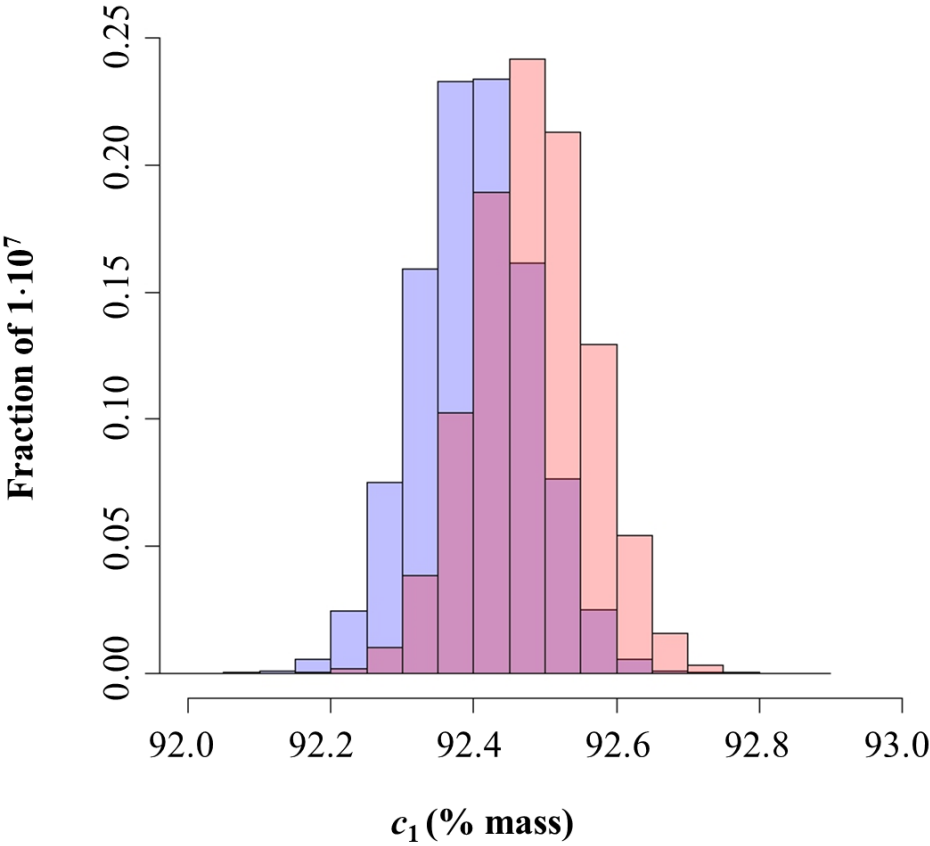
Histogram of the marginal pdf of the Pt content, c_1. Pink values represent the distribution of Pt content before closure operation, whereas blue values - after this operation taking into account the mass balance constraint.

1

Correlation of test results and influence of a mass balance constraint on risks in conformity assessment of a substance or material

Francesca R. Pennecchi[a], Aglaia Di Rocco[b], Ilya Kuselman[c,*], D. Brynn Hibbert[d] and
Michela Sega[a]

[a] Istituto Nazionale di Ricerca Metrologica (INRIM), Strada delle Cacce 91, 10135 Turin, Italy

[b] University of Turin, Via Verdi 8, 10124, Turin, Italy

[c] Independent Consultant on Metrology, 4/6 Yarehim St., 7176419 Modiin, Israel

[d] School of Chemistry, UNSW Sydney, Sydney NSW 2052, Australia

----

* Corresponding author. Tel.: +972-50-6240466

E-mail address: ilya.kuselman@bezeqint.net (I. Kuselman).

4/6 Yarehim St., Modiin, 7176419 Israel

2

ABSTRACT

When components of a substance or material are subject to a mass balance constraint, test results of the components' contents are intrinsically correlated because of the constraint. That is in addition to possible metrologically-related correlation of test results, and natural and/or technological correlation of the components' contents. Such correlations may influence understanding of compositional data and evaluation of risks in conformity assessment of the substance or material due to measurement uncertainty. A Bayesian multivariate approach to evaluate the conformance probability of multicomponent materials or objects and corresponding risks of false decisions, able to take into account all observed correlations including spurious, is discussed for different scenarios of compositional data. A Monte Carlo method, which includes the mass balance constraint, written in the R programming environment is provided for the necessary calculations. A technique for separation of spurious correlations from experimental (natural and/or technological) correlations is proposed.

1. Introduction

A number of techniques are used during development of a chemical analytical method to overcome possible correlations between test/measurement results of concentrations or contents of different components (main as well as impurities) of a substance or material. Some of these techniques include extraction of target components (analytes) from a sample and chromatographic separation of an analyte from other components of the sample [1]. Chemometrics software is applied for separation of spectral signals and multivariate calibrations of spectrometers [2]. Sample digestion [3] and standard additions of an analyte to a sample [4] are used for calibration of a measuring system to overcome multiplicative matrix effects, and so on. There are validation requirements for "analytical selectivity" of a standard operating procedure (SOP), as its performance characteristic, to prove the procedure's fitness for purpose. IUPAC Recommendations [5] and the Eurachem Guide [6] define that "analytical selectivity relates to the extent to which the method can be used to determine particular analytes in mixtures or matrices without interferences from other components of similar behavior". This definition is consistent with "selectivity of a measuring system" in JCGM 200 [7]. The corresponding procedure validation parameter in the pharmaceutical industry is termed in ICH Guideline [8] "specificity". A procedure not able to answer the requirements of selectivity or specificity is not 'fit-for-purpose' and cannot be applied to the given task. Validation of the SOP, training analysts and proficiency testing, supervision and quality control are elements of the quality system of an analytical laboratory that should prevent human error causing metrologically–related correlation, unless, as shown in Fig. 1, the Swiss-cheese model [9] lines up an error in each element. Therefore, correlations that have arisen in the routine measurement process should be in general negligible and test results for two or more components of the same item (sample) are expected to be metrologically independent. In practice, if statistically significant correlation between measured values of concentrations or contents of components of the same sample is detected, analysis cannot be continued without a thorough chemical analytical inspection of the reason for the correlation in the laboratory. For example, when a medication is tested routinely with a pharmacopeial HPLC procedure, correlations might be related to the resolution of the chromatography column used, not able to separate the analytes completely, and the column must be replaced by another one. In the IUPAC/CITAC Guide [9] such an event is rated as a skill-based mistake or omission error (lapse).

However, test results of chemical compositions of different batches, lots or objects are inevitably correlated when their actual ("true") values are correlated. Correlations of contents of sample components can be caused by natural physicochemical properties of substances, such as stoichiometry [10-12], and by technological reasons in a material production [13, 14]. These correlations are taken into account using "conventional" multivariate statistical methods.

When components $i = 1, 2, …, n$ of a substance or material are subject to a mass balance constraint (sum of their contents c_i - mass fractions, mole fractions or any other positive quantity ratios - is 100 % or 1), test results of the components' contents are called "compositional data". These data are intrinsically correlated because of the constraint, and the relevant correlation was named by Karl Pearson in 1897 as "spurious" [15-17]. It is a kind of mathematical property of the data, not related to physicochemical interdependence of true values of contents of a material component. Compositional data may be depicted in a multi-dimensional simplex, as in Fig. 2, in which, in general, Euclidean geometry cannot be blindly applied. Compositional Data Analysis (CoDA) based on an isometric logratio transformation of the original test results was developed in the 1980's by John Aitchison [18-20]. Logratios of amalgamations of test results for pairs of components (parts of the data) – pairwise logratios – were recently used for practical simplification of CoDA [21-24]. There are a number of examples of CoDA applications in geochemistry [25, 26], agriculture and environmental analysis [27-30], bioinformatics [31, 32], forensic science [33, 34], materials [35], and other fields. More publication references, software, slides and lecture notes can be found at website CODAWEB [36].

There is also a strong message in the literature (e.g., in refs. [25, 26, 37]) stressing how traditional statistical techniques may produce inadequate results if applied to raw compositional data without suitable transformation. However, the relevant techniques of CoDA are still not implemented widely, neither in metrology in chemistry nor in conformity assessment. Spurious correlations may influence evaluation of measurement uncertainty of compositional data (e.g. of standard gas mixtures [38, 39]) and quantification of risks of false decisions due to measurement uncertainty in the conformity assessment of a substance or material. A special case is characterization of materials based on a mass balance [40-43], for example matrix reference materials, as well as evaluation of purity of substances and corresponding (pure) certified reference materials.

5

A multivariate Bayesian model was recently elaborated for evaluation of risks of false decisions in conformity assessment of multicomponent materials or objects, also taking into account possible correlations between measured concentrations or contents of an item's components [13, 14, 44-47]. This "conventional" approach applies integration of the relevant posterior multivariate probability density function on the tolerance/specification multi-domain of the material (or object) compositions in order to obtain total specific risks, or integration of the joint probability density function of true and measured values to give total global risks. All observed correlations are embedded in the corresponding experimental covariance matrix. This matrix influences the subsequent multivariate results.

A problem of application of CoDA in this field is that a subset of the components may not be related directly to the mass balance, i.e. be outside of the multidimensional simplex; for example, when a sum of impurities' contents is a member of the mass balance, but individual impurities or a subset of those impurities also have to undergo conformity assessment. Since each component participating in conformity assessment has content tolerance/specification limits, the mass balance constraint forms a multivariate sub-domain of the feasible material or object compositions in the domain of specification limits. Moreover, spurious correlation coefficients may be comparable or smaller (in absolute values) than coefficients of correlations caused by natural properties of the materials and technological reasons [14], and in general be not easily distinguishable from them. In addition, using isometric logratio transformation of data, it might be difficult to interpret relevant estimates for conformity assessment purposes in the original variable space.

In this regard, a new IUPAC project [48] was started with the aim of developing guidelines for treatment of influence of a mass balance constraint on measurement uncertainty of test results of a substance or material and risks in its conformity assessment. In the present position paper of the project, a Bayesian multivariate approach for evaluating the probability of conformance of a substance or material and the risks of false decisions is discussed for different scenarios of compositional data. A Monte Carlo method, which includes the mass balance constraint, written in the R programming environment, is developed for the necessary calculations. A technique for separation of spurious correlations from experimental (natural and/or technological) correlations is also proposed.

2. A Bayesian multivariate approach to conformity assessment of compositional data

The chemical composition of a material or substance is considered to conform when the actual ("true") value of the content c_i of each i-th component under control, $i = 1, 2, \ldots, n$, is within its tolerance (specification) interval $T_i = [T_{Li}, T_{Ui}]$, where T_{Li} and T_{Ui} are lower and upper tolerance limits of the interval, respectively. The term "component" relates to a main component or an impurity or a group of impurities in the item (sample, batch or lot). To decide whether the material or substance conforms or not, the measured content value c_{im} is compared with the limits of the acceptance interval $A_i = [A_{Li}, A_{Ui}]$, where A_{Li} and A_{Ui} are lower and upper limits of the interval, respectively, taking into account the standard measurement uncertainty u_i associated with c_{im}. This uncertainty causes risks of a false decision on conformity [49].

2.1. Compositional data properties

The vector of measured values $\boldsymbol{c_m} = [c_{1m}, c_{2m}, \ldots, c_{nm}]$ describes the n-component (n-part) composition of a material or substance. The compositional data space is the simplex

$$S^n = \{\boldsymbol{c_m} = [c_{1m}, c_{2m}, \ldots, c_{nm}] \mid c_{im} > 0, \ i = 1, 2, \ldots, n; \ \sum_{i=1}^{n} c_{im} = k\}, \tag{1}$$

where k is usually equal to 1 or 100 %, but might be any other positive constant value. As c_{im} are positive quantity ratios, a vector of measured values $\boldsymbol{c_m}$ multiplied by any positive constant contains the same information as the original one, i.e. represents the same composition and can be considered as an equivalence class. This property is termed "scale invariance". In other words, if $\boldsymbol{c_m}$ is scaled by a constant, e.g. measured content values c_{im} changing from parts-per-unit to percentages, the information which $\boldsymbol{c_m}$ conveys is completely equivalent. Therefore, it is natural to select a representative of the equivalence class to facilitate data analysis and interpretation of corresponding results. This selection is formalized by the closure operation:

$$clo\ (\boldsymbol{c_m}) = \left[\frac{k \cdot c_{1m}}{\sum_{i=1}^{n} c_{im}}, \ldots, \frac{k \cdot c_{nm}}{\sum_{i=1}^{n} c_{im}}\right]. \tag{2}$$

Compositional data do not depend on the order of measured contents c_{im} within vector $\boldsymbol{c_m}$. The order does not influence conclusions of any analysis on $\boldsymbol{c_m}$. This is known as the "permutation invariance" property. Another property is "subcompositional coherence", which means that analyses concerning a subset of the component contents should not depend on the remaining part. If a metric is used to compare two compositions on the simplex, the distance between the two should be greater than or equal to that obtained comparing any couple of corresponding subcompositions. That is called "subcompositional dominance". This property is used to measure distances between compositions and subcompositions following the rule of a projection: distances become smaller in a projection.

Note, ordinary correlations (natural and/or technological) depend on the subcomposition considered and violate subcompositional coherence. The ordinary Euclidean distance between the vectors cannot be evaluated here, as both scale invariance and subcompositional dominance are violated [18].

2.2. Modelling composition of a material or substance

Vector $\boldsymbol{c} = \left[c_1, c_2, \ldots, c_n\right]$ represents the actual ("true") n-component composition of a material or substance. Component contents c_i, $i = 1, 2, \ldots, n$, are the measurands in conformity assessment, and $\boldsymbol{c}$ is the vector of the measurands. Using a multivariate Bayesian approach [13, 14, 44-47], knowledge about a composition $\boldsymbol{c}$ can be modelled by a random multivariate posterior variable and expressed in terms of its probability density function (pdf). Such a pdf combines prior knowledge about the measurands and new information acquired during the measurements:

$$g\left(\boldsymbol{c} \,|\, \boldsymbol{c}_m\right) = C g_0(\boldsymbol{c}) h\left(\boldsymbol{c}_m \,|\, \boldsymbol{c}\right), \tag{3}$$

where $g(c \mid c_{\mathrm{m}})$ is the posterior pdf; C is a normalizing constant; $g_0(c)$ is the multivariate prior pdf; and $h(c_{\mathrm{m}} \mid c)$ is the multivariate likelihood function taking into account the measurement uncertainties and possible covariance terms.

A large enough dataset of results of testing items of the same material produced at the same factory, or results of monitoring the same environmental compartment, can be used for modelling the prior pdf $g_0(c)$. The assumption is that the actual content values are approximated by the test/measurement results adequately, since measurement uncertainty is negligible in comparison with item-to-item (batch-to-batch) variations caused by changes of conditions of the material production, environmental conditions, etc. Based on this assumption, normal and gamma distributions in JCGM 106 [49], as well as normal, lognormal and Weibull distributions in IUPAC/CITAC Guide [50], were considered as prior pdfs in univariate conformity assessment. Multivariate normal distributions in refs. [13, 14], normal and lognormal distributions in refs. [44, 45] were used in conformity assessment of materials and an environmental object.

If there is no detailed prior knowledge about distribution of the component content in the tested items, the prior pdf is vague. According to the principle of maximum entropy, a multivariate normal distribution is usually considered as the joint prior pdf for the vector of actual component contents c when the mean μ and covariance matrix V constitute the only available information about the vector quantity [51]. In case of compositional data c, however, their properties need to be taken into account when assigning a corresponding pdf. Since the vector c is non-negative, and the first two moments of the distribution (the expected value and variance) are known, the maximum entropy distribution is a truncated multivariate normal distribution, not a logarithmic one [52]. This is also the case for an elliptical truncation region [53], when the pdf is supposed to be nonzero-valued just for $(c - \mu)^{\mathrm{T}} V^{-1}(c - \mu) \le k$.

Therefore, in the present work, a truncated multivariate normal (TMN) distribution on the nD region $[0, k]^n$ is employed in modelling the prior pdf of c. It is written TMN(μ,V), μ and V being the location and scale parameter, respectively, of the original normal pdf from which the TMN distribution arises by truncation on $[0, k]^n$. For the univariate case, the TMN pdf for c_i on the interval $[0, k]$ is

$$f_i = \frac{\phi\left(\frac{c_i - \mu_i}{\sigma_i}\right)}{\sigma_i\left(\Phi\left(\frac{k - \mu_i}{\sigma_i}\right) - \Phi\left(\frac{-\mu_i}{\sigma_i}\right)\right)}, \tag{4}$$

where μ_i and σ_i are the mean and standard deviation (the location and scale parameters) of the normal pdf from which this TMN distribution arises; $\phi(\cdot)$ is the pdf of the standard normal distribution and $\Phi(\cdot)$ is its cumulative distribution function. Outside the interval $[0, k]$, the pdf f_i is equal to zero.

Accordingly, the likelihood function $h(\boldsymbol{c}_m | \boldsymbol{c})$ can be also modelled on the base of a TMN of the measured values, having location parameter equal to the vector $\boldsymbol{c}$ of actual/"true" values, i.e. TMN($\boldsymbol{c}, \boldsymbol{U}$), where $\boldsymbol{U}$ is the covariance matrix of measurement uncertainties u_i and covariance terms u_{ij} whose corresponding correlation coefficients are the same as for $\boldsymbol{V}$. Correlation between measured content values c_{im} and c_{jm} is the same as between the corresponding actual ones c_i and c_j, when no other (metrologically-related) correlation arose in the measurement process.

The multivariate truncated distribution accommodates the constraint of compositional data to lie on the region $[0, k]^n$ and is promising for overcoming the above-mentioned problems of application of CoDA for evaluation of risks of false decisions in conformity assessment.

2.3. Models for the prior distribution

Let us consider the case of $c_1 + c_2 + c_3 = 100\%$, or without loss of generality $c_1 = 100\% - c_2 - c_3$. As an example, the composition of a PtRh alloy described in paper [14] is discussed below. Here, c_1 is the Pt content in the PtRh alloy, c_2 is the Rh content, and c_3 is the content of eight impurities (sum of their mass fractions). Prior means μ_i and standard deviations σ_i, as well as observed correlation coefficients r_{ij}, $i \neq j$, for these three components are shown in Table 1. The content of an additional component of the alloy that is under control in conformity assessment – the sum of mass fractions of the three precious impurities (a part of c_3) – is not considered here as it is not related directly to the mass balance.

The following scenarios have been considered for modelling the multivariate prior probability distribution of the actual ("true") three-component composition described by the vector $\boldsymbol{c}$:

1) <u>Modelling all the actual values of the components' contents</u>: the closure operation $clo(\boldsymbol{c})$ is applied to $\boldsymbol{c}$ following a TMN($\boldsymbol{\mu}, \boldsymbol{V}$) distribution on the 3D region $[0, 100]^3$.

2) <u>Modelling actual values of two components' contents and deriving the third</u>: $[c_2, c_3]$ follows a bivariate TMN($\boldsymbol{\mu}_{23}, \boldsymbol{V}_{23}$) distribution on the 2D region $[0, 100]^2$, where subscript

"23" indicates that the applied operation refers just to components 2 and 3. The scale parameter V_{23} involves the correlation coefficient $r_{23} = 0.228$, and c_1 is deterministically calculated as $c_1 = 100\ \% - c_2 - c_3$, disregarding possible negative values.

3) <u>Sequential modelling</u>: c_2 follows a $TN(\mu_2,\sigma_2)$, a univariate normal distribution truncated on the interval [0, 100]; $c_3|c_2$ has a conditional probability distribution following a $TN(\mu_3,\sigma_3)$ on the interval [0, $100 - c_2$]; and, again deterministically, $c_1|(c_2, c_3) = 100\ \% - c_2 - c_3$.

In order to assess the suitability of the models, two parameters are considered: 1) the correlation matrix encompassing correlation coefficients r_{ij} of the multivariate prior pdf, and 2) the pdf coverage probability p, calculated as its integral over the multivariate tolerance region, which is [92.2 %, 92.8 %] × [7.3 %, 7.7 %] × [0 %, 0.18 %] for the present example. By definition, p is the probability that the prior values of all the three variables lie within corresponding tolerance intervals. The calculation of p using the Monte Carlo (MC) method is described in Appendix 1. Equivalence or dissimilarity of this parameter's values from model to model indicate that the multivariate pdfs generated by the various models are actually the same or different, respectively. Results of calculating r_{ij} and p obtained by means of 10^7 MC simulations for each model, are reported in Table 2. For comparison, $p = 0.979$ was obtained when the ordinary multivariate normal distribution was applied in ref. [14] and the original/experimental correlation coefficients shown in Table 1 were used.

Table 2

Correlation coefficients in Table 2 for the prior pdf obtained by models 1 and 2 are equal, within the precision of the MC simulation, to the experimental ones in Table 1, considering that two decimal digits in the coefficient estimates can be taken as reliable when 10^7 MC simulations are performed. For both models 1 and 2, coverage probabilities slightly greater than $p = 0.979$ are obtained, meaning that the prior pdfs generated by these models are narrower than the ordinary multivariate normal pdf.

To show the influence of the closure operation on a TMN pdf, boxplots of the marginal pdfs of the three variables by model 1, before the closure operation (boxplot 1) and after it (boxplot 2), are depicted in Fig. 3. The closure operation shifts the marginal pdf location towards smaller values, especially for c_1, i.e. the Pt content. More details of this pdf are shown in the histogram of c_1 in Fig. 4.

Fig. 3

Fig. 4

By model 3, the contents of Rh (c_2) and the impurities (c_3) are each drawn from a univariate truncated normal distribution, one of which depends on the other just in its truncation limits. Pt content values are deterministically generated to satisfy the mass balance constraint. In this model, there is no place for a covariance matrix encompassing the correlation coefficients which reflect different kinds of correlation between the contents. The correlation matrix by model 3 can reveal only the spurious correlations arising from the truncation effect and the mass balance constraint. In the present example, as the sum of Rh and impurities contents is always far away from 100 %, correlation between the two due to the truncation effect is negligible. Thus, the correlation coefficient arising from spurious correlations between Rh and the impurities contents is zero, despite the fact that the experimental correlation coefficient is 0.288. Also, the spurious correlation coefficient for Pt and the impurities contents is different from the observed correlation coefficient, due to both the mass balance constraint and the nature of the raw materials. Nonetheless, the coverage probability obtained for model 3 is very close or equal to those by models 1 and 2.

In general, modelling 1 is suitable for matrix reference materials, standard gas mixtures, food products, etc., i.e. for materials whose composition is tested completely and the test results should correspond to a mass balance. Modelling 2 can be applied for pure substances or materials in which the main component content is not tested using physicochemical measurement methods but calculated based on a mass balance constraint. Sequential modelling 3 is more complicated, since the sequence of c_2 and c_3 can be exchanged and that may lead to different results as the conditional probabilities are different. Moreover, the number of such models increases significantly with the number of components $n > 3$. This modelling does not allow consideration of types of correlation other than spurious and cannot be implemented adequately when natural (stoichiometric) and/or technological correlations are significant. On the other hand, modelling 3 could be a helpful tool for understanding sources of the experimental correlation, disentangling its spurious part from the rest.

2.4. Likelihood modelling for a component content calculated based on a mass balance constraint

According to the propagation of uncertainty prescribed by JCGM 100 [55] for correlated input quantities, when contents of a main component ($i = 1$) are calculated based on a mass balance

constraint $c_1 = 100\ \% - \sum_{i=2}^{n} c_i$, the squared measurement uncertainty associated with the calculated c_{1m} is

$$u_1^2 = \sum_{i=2}^{n} u_i^2 + 2\sum_{i=2}^{n}\sum_{j=i+1}^{n} u_i u_j r_{ij}. \tag{5}$$

In the example of the three components of the PtRh alloy participating in the mass balance, the standard measurement uncertainty u_1 associated with the calculated Pt content c_{1m} is evaluated as following:

$$u_1 = (u_2^2 + u_3^2 + 2u_2 u_3 r_{23})^{0.5} = (0.040^2 + 0.011^2 + 2 \cdot 0.040 \cdot 0.011 \cdot 0.228)^{0.5} = 0.044\ (\%),$$

where $u_2 = 0.040\ \%$ is the standard uncertainty associated with the measured Rh content c_{2m} in its tolerance (specification) interval, and $u_3 = 0.011\ \%$ is the standard measurement uncertainty associated with the measured mean of the impurities content $c_{3m} = 0.059\ \%$ (the relative standard uncertainty being $u_3/c_{3m} = 0.18$). When correlation between contents of components 2 and 3 is ignored, e.g. in model 3 where $r_{23} = 0$, the measurement uncertainty associated with the calculated c_{1m} is $u_1 = 0.041\ \%$.

The modelling of the likelihood function for measured content values $\boldsymbol{c_m}$ is based on the idea that an appropriate pdf with zero expectation is chosen for an error $\boldsymbol{e_m}$ and then translated to the vector of actual ("true") content values $\boldsymbol{c}$ generated for the prior. Therefore, $\boldsymbol{c_m}$ is recovered as $\boldsymbol{c_m} = \boldsymbol{c} + \boldsymbol{e_m}$. The covariance matrix $\boldsymbol{U}$ associated with $\boldsymbol{c_m}$ contains the squared above-mentioned uncertainties u_i and the covariance terms u_{ij} whose corresponding correlation coefficients are the same as for $\boldsymbol{V}$. The error $\boldsymbol{e_m}$ pdf, having zero mean, is the same as that for the likelihood when translated into the vector $\boldsymbol{c}$. The truncation limits are chosen such that each component of the vector $\boldsymbol{c_m}$ has to be between zero and 100 %: $\boldsymbol{0}\ \% < \boldsymbol{c_m} = \boldsymbol{c} + \boldsymbol{e_m} < \boldsymbol{100}\ \%$. Hence, a vector of errors is extracted between $-\boldsymbol{c}$ % and $(\boldsymbol{100} - \boldsymbol{c})$ %, where $\boldsymbol{c}$ is drawn from the prior pdf. For ease of computation, the $\boldsymbol{c}$ values in these truncation limits are approximated with corresponding mean values $\boldsymbol{\mu}$. Thus, the modelling of the likelihood follows that of the prior:

    1) <u>Modelling the likelihood of all the measured component contents</u>: $\boldsymbol{e_m}|\boldsymbol{c}$ is used as a TMN($\boldsymbol{0}, \boldsymbol{U}$) distribution on the region $[-\mu_1,\ 100 - \mu_1]$ % $\times\ [-\mu_2,\ 100 - \mu_2]$ % $\times\ [-\mu_3,$

$100 - \mu_3$] % for the c_{m} generation, where c is approximated by μ, and then applying the closure operation $clo(c_{\mathrm{m}})$.

2) Modelling the likelihood of two measured component contents and deriving the third: $[e_{2\mathrm{m}}, e_{3\mathrm{m}}]|c_{23}$ is taken as a bivariate TMN($0, U_{23}$) distribution on the region $[-\mu_2, 100 - \mu_2]$ % $\times [-\mu_3, 100 - \mu_3]$ % for the $c_{2\mathrm{m}}$ and $c_{3\mathrm{m}}$ generation, where c_{23} is approximated by μ_{23}, and U_{23} involves the correlation coefficient $r_{23} = 0.228$. Then, $c_{1\mathrm{m}} = 100$ % $- c_{2\mathrm{m}} - c_{3\mathrm{m}}$ is calculated directly, disregarding its possible negative values.

3) Sequential modelling the likelihood: $e_{2\mathrm{m}}|c_2$ is represented by a univariate TN($0, u_2$) distribution on $[-\mu_2, 100 - \mu_2]$ % interval for the $c_{2\mathrm{m}}$ generation, where c_2 is approximated by μ_2, and $e_{3\mathrm{m}}|c_{23}$ by a univariate TN($0, u_3$) on the interval $[-\mu_3, 100 - \mu_3 - c_{2\mathrm{m}}]$ % for the $c_{3\mathrm{m}}$ generation, where c_3 is approximated by μ_3. Then, $c_{1\mathrm{m}} = 100$ % $- c_{2\mathrm{m}} - c_{3\mathrm{m}}$ is calculated directly, as in the previous modelling.

When the prior pdf and likelihood function are modelled, the joint pdf for true and measured values given by the product $g_0(c)h(c_{\mathrm{m}}|c)$, and the posterior pdf for the measurand c may be obtained by eqn. (3). Thus, evaluation of risks in conformity assessment of a material or substance, using compositional data, is possible.

3. Risks in conformity assessment of compositional data

3.1. Kinds of risks

Several kinds of risk of a false decision on conformity of an item due to measurement uncertainty may be evaluated. The probability of accepting a batch of the material, when it should be rejected, is the 'consumer's risk', whereas the probability of falsely rejecting the batch is the 'producer's risk'. For a specified batch, they are referred to as the 'specific consumer's risk' R_{ci}^* and the 'specific producer's risk' R_{pi}^*, respectively, for the i-th particular component of the material under control [49]:

$$R_{ci}^* = \int_{T_i^c} g(c_i \mid c_{i\mathrm{m}}) dc_i \quad \text{and} \quad R_{pi}^* = \int_{T_i} g(c_i \mid c_{i\mathrm{m}}) dc_i, \tag{6}$$

where T_i^c is the interval complementary to the tolerance (specification) interval T_i, and measured value c_{im} is inside of the acceptance interval in the case of R_{ci}^* and outside — in the case of R_{pi}^*. Thus, R_{ci}^* relates to the situation when a batch is accepted at the value c_i out of T_i, while R_{pi}^* - when a batch is rejected at c_i in T_i.

The risks of incorrect conformity assessment of a batch randomly drawn from a statistical population of such batches are the 'global consumer's risk' R_{ci} and the 'global producer's risk' R_{pi}, respectively, as they characterize the material production globally [49]:

$$R_{ci} = \int_{T_i^c} \int_{A_i} g_0(c_i) h(c_{im} \mid c_i)\, dc_{im} dc_i \quad \text{and} \quad R_{pi} = \int_{T_i} \int_{A_i^c} g_0(c_i) h(c_{im} \mid c_i)\, dc_{im} dc_i, \qquad (7)$$

where A_i^c is the interval complementary to the acceptance interval A_i.

When conformity assessment for each i-th component of a material is successful (i.e. the particular specific or global risks are small enough), the total probability of a false decision concerning the material as a whole (the *total* specific R^* or *total* global R risk) might still be significant. The total risks are also consumer's and producer's, as shown below with subscripts "c" and "p", respectively:

$$R_c^* = \int_{T^c} g(c \mid c_m) dc \text{ (for } c_m \text{ in } A) \text{ and } R_p^* = \int_T g(c \mid c_m) dc \text{ (for } c_m \text{ outside } A), \qquad (8)$$

$$R_c = \int_{T^c} \int_A g_0(c) h(c_m \mid c)\, dc_m dc \text{ and } R_p = \int_T \int_{A^c} g_0(c) h(c_m \mid c)\, dc_m dc, \qquad (9)$$

where T is the tolerance region $T_1 \times T_2 \times \ldots \times T_n$; A is the acceptance region $A_1 \times A_2 \times \ldots \times A_n$; and superscript "c" means "complementary".

Altogether, for $n > 1$ components under control, one can distinguish $4(n+1)$ kinds of risks of false decisions [56]. Evaluation of the total global risks of false decisions on the conformity of compositional data (constrained by a mass balance) using a Monte Carlo method in the R programming environment is discussed below. Quantification of total specific risks will be addressed in the framework of the project [48] at a subsequent stage.

3.2. Evaluation of the total global risks

To evaluate the global risks in the case of three variables related to a mass balance, prior pdf and likelihood function are modelled as in sections 2.3 and 2.4, respectively. Then, 10^7 MC simulations of the joint pdf $g_0(c)h(c_m|c)$ are generated simulating prior values from $g_0(c)$ and corresponding likelihood values from $h(c_m|c)$. The three models for the prior and likelihood discussed in the previous section give three ways to obtain the joint pdf. The function "rtmvnorm" [57] is applied in the first and the second model, and the function "rtnorm" [58] in the third model. Finally, the joint pdf is represented by values of the vector $[c_1, c_2, c_3, c_{1m}, c_{2m}, c_{3m}]$.

The total producer's risk R_p is evaluated considering the fraction of the number of cases (from the total number of 10^7 MC simulations) when all the actual values c_1, c_2, c_3 are within the corresponding tolerance region T, while at least one of the measured values c_{1m}, c_{2m}, c_{3m} is out of its acceptance interval A_i, $i = 1, 2, 3$, respectively. The total consumer's risk R_c is evaluated as the fraction of the number of cases when all the measured values c_{1m}, c_{2m}, c_{3m} are within the acceptance region A, while at least one of the actual values c_1, c_2, c_3 is out of its tolerance interval T_i, $i = 1, 2, 3$, respectively. Core calculations of the developed R code are presented in Appendix B.

For the three discussed models, the total global consumer's risk at the acceptance limits equal to the tolerance limits ($A = T$) was the same $R_c = 4.7 \times 10^{-3}$. A similar result $R_c = 5.1 \times 10^{-3}$ was reported in the paper [14] for a scenario when Pt, Rh and the eight impurities contents only were taken into account: the slight difference in the risk values is due to different numerical implementations of the risk calculation. For more details, the R_c dependence on A_2 and A_3 (at $A_1 = T_1$) was also studied, as shown in Fig. 5a for model 1. The arrows on both the plots in Fig. 5 show

the acceptance intervals from $A_2 = T_2$ and $A_3 = T_3$, at the beginning of the axes, to the acceptance intervals with limits differing from the tolerance limits by three times the relevant measurement uncertainty ($3u_i$), at the axes' ends. Specifically, in Fig. 5a, these are the lower acceptance limit $A_{L2} = T_{L2} + 3u_2 = 7.3 + 3 \times 0.04 = 7.42$ (%) and the upper acceptance limit $A_{U2} = T_{U2} - 3u_2 = 7.7 - 3 \times 0.04 = 7.58$ (%). Since the upper only tolerance limit T_{U3} is set for the content of the impurities, at the end of the A_3 axis $A_{L3} = 0$ and $A_{U3} = T_{U3} - 3u_3 = 0.18 - 3 \times (0.059 \times 0.18) = 0.15$ (%), where 0.059 % is the value of the content prior mean μ_3 of the impurities (Table 1). The color column bar in the plot gives indication of the risk R_c values between the minimum and the maximum on the surface, from 3×10^{-6} to 4.7×10^{-3}. One can see on the plot that the influence of the impurities'

content on the risk is negligible under these conditions. That is because the content prior mean μ_3 = 0.059 % is far enough from the tolerance limit T_{U3} = 0.18 %.

The dependences of R_c on the acceptance intervals for the second and the third models are very similar (R_c varying from 4×10^{-6} to 4.7×10^{-3} and R_c from 6×10^{-6} to 4.6×10^{-3}, respectively). These results show that the mass balance influence on R_c in the small sub-domain of feasible alloy compositions is practically negligible.

The total global producer's risk at $A = T$ was R_p = 2.4×10^{-2} for models 1 and 2, and a bit smaller R_p = 2.0×10^{-2} for model 3. The producer's risk values were not discussed in ref. [14] but have been calculated, for sake of comparison, according to the approach proposed there, leading to the same value R_p = 2.4×10^{-2}. The R_p dependence on A_2 and A_3 (at $A_1 = T_1$) is presented for model 1 in Fig. 5b, where, at the end of the axes, $A_{L2} = T_{L2} - 3u_2 = 7.3 - 3\times0.04 = 7.18$ (%) and $A_{U2} = T_{U2}$

Fig. 6

$+ 3u_2 = 7.7 + 3\times0.04 = 7.82$ (%), and $A_{L3} = 0$ and $A_{U3} = T_{U3} + 3u_3 = 0.18 + 3\times(0.059\times0.18) = 0.21$ (%), respectively. The color column bar gives indication of R_p values from 4.9×10^{-3} to 2.4×10^{-2}. The influence of the impurities' content on the producer's risk is minor at these conditions, as it is for the consumer's risk for the same reason.

The dependence of R_p on the acceptance intervals for the second model is very similar as well, its values being practically the same: R_p from 4.8×10^{-3} to 2.4×10^{-3}. However, the third model produces smaller values of R_p from 3.7×10^{-4} to 2.0×10^{-3}.

The obtained results show that the mass balance influence on the consumer's and producer's risks, evaluated with models 1 and 2, is not visible in the small sub-domain of feasible alloy compositions. The plots by these two models, like in Fig. 5, allow choice of acceptance limits corresponding to the suitable risks of the consumer(s) and the producer. The departure of results by model 3, with respect to the results obtained with models 1 and 2, is caused by the fact that model 3 does not take into account correlations other than spurious (natural and technological). Therefore, this model is helpful not only to separate spurious correlation from the observed/experimental (cumulative) correlation, but also to indicate how significant the difference between them in a material conformity assessment is.

4. Conclusions

Three kinds of correlation can be considered between components' contents of a substance or material which meet requirements of a mass balance: 1) metrologically-related, 2) natural and technological, and 3) spurious. All these kinds of correlation have been taken into account in the Bayesian multivariate approach modified for evaluating the conformance probability of a substance or material and the risks of false decisions in its conformity assessment when the material components' contents satisfy a mass balance constraint.

Three models of prior pdfs and likelihood functions describing the compositional data in the framework of the Bayesian multivariate approach can be applied. Model 1 is suitable for materials whose composition is tested completely and for which the test results should correspond to a mass balance. Model 2 can be applied for testing pure substances or materials in which the main component content is not measured using physicochemical measurement methods, but calculated based on a mass balance constraint. Model 3 is a helpful tool for understanding sources of experimental correlation, disentangling the spurious part from natural and/or technological correlations.

A Monte Carlo method, coded in the R programming environment, was developed for calculations of the coverage probability of the prior pdf and the total global risks of false decisions on conformity of a material or substance, taking into account the mass balance constraint of the data.

The approach to conformity assessment of compositional data is demonstrated using an example of a PtRh alloy, for which spurious correlation effects were minor.

Acknowledgement

Appendix A. Evaluation of coverage probability

Evaluation of the coverage probabilities for three variables according to the models of prior pdfs described in sec. 2.3 was performed in the R programming environment using the library "compositions" [59] and a Monte Carlo method with 10^7 simulations.

For the first model, where c follows a TMN(μ,V) distribution on the region $[0, 100]^3$, a prior pdf as a trivariate truncated normal distribution was generated using the function "rtmvnorm" with truncation limits equal to $[0, 0, 0]$ and $[100, 100, 100]$. Note, a non-singular matrix is inserted as an approximation of matrix V. Then, the function "clo" was applied for performing the closure operation with the constraint equal to 100 %.

For the second model the function "rtmvnorm" was applied to generate a bivariate truncated normal distribution with truncation limits $[0, 0]$ and $[100, 100]$. Then, the third variable was computed as $c_1|(c_2, c_3) = 100\ \% - c_2 - c_3$. Rows $[c_1, c_2, c_3]$ of the matrix, containing negative generated values of the third component content, were removed.

In the third model, c_2 is generated using the function "rtnorm" with the truncation lower limit 0 % and the upper limit 100 %. Then, variable $c_3|c_2$ was given by the same function, "rtnorm", but with the truncation limits 0 % and 100 % $- c_2$, i.e. for each value of c_2 the corresponding value of c_3 was in the interval $[0, 100 - c_2]$. In this way $0 < c_{2+}c_3|c_2 < 100$. Finally, the third variable was computed as $c_1|(c_2, c_3) = 100\ \% - c_2 - c_3$.

When the prior pdf is generated in the form of a matrix containing rows of values $[c_1, c_2, c_3]$, the coverage probability can be evaluated using function "length" to count cases where c_1, c_2 and c_3 values are simultaneously within their limits. For each row corresponding to this condition, the function gives the number 3, because three variables were treated. Thus, to obtain the coverage probability, the result of the "length" function should be divided by 3×10^7. One can also compute marginal coverage probability, taking into account the variables one by one. Core calculations of the developed R code are presented in Appendix B.

Appendix B. Core calculations of the R code

B.1. Calculation of the coverage probability of the prior pdf

```
library(mvtnorm)
library(msm)
library(tmvtnorm)
library(compositions)
library(nortest)

rm(list=ls())
```

```
# Tolerance limits
lrl1 = 92.2
url1 = 92.8
lrl2 = 7.3
url2 = 7.7
lrl3 = 0
url3 = 0.18


###########
# MODEL 1

n = 10000000
mu1 = 92.483
mu2 = 7.547
mu3 = 0.059
uc1 = 0.081
uc2 = 0.073
uc3 = 0.021
mean = c(mu1,mu2,mu3)
sigma = matrix(c(uc1^2,-0.967*uc1*uc2,-0.467*uc1*uc3,-
0.967*uc1*uc2,uc2^2,0.228*uc2*uc3,-0.467*uc1*uc3,0.228*uc2*uc3,uc3^2), nrow = 3)
lower = rep(0,3)
upper = rep(100, 3)

priorTMN = rtmvnorm(n, mean = mean, sigma = sigma, lower, upper)
prior = clo(priorTMN, total=100)

prior1 = prior[,1]
prior2 = prior[,2]
prior3 = prior[,3]

# Correlation matrix of the modelled multivariate prior PDF
cor(cbind(prior1, prior2, prior3))

# Joint coverage probability
Pcov123 = length(prior[(prior1>=lrl1 & prior1<=url1) & (prior2>=lrl2 & prior2<=url2) &
(prior3>=lrl3 & prior3<=url3)])/(3*n)
Pcov123

# X Marginal coverage probability
Pcov1 = length(prior1[prior1>=lrl1 & prior1<=url1])/n
Pcov1

# Y Marginal coverage probability
Pcov2 = length(prior2[prior2>=lrl2 & prior2<=url2])/n
```

20

Pcov2

```
# Z Marginal coverage probability
Pcov3 = length(prior3[prior3>=lrl3 & prior3<=url3])/n
Pcov3
```


```
############
# MODEL 2

n = 10000000
mu2 = 7.547
mu3 = 0.059
uc2 = 0.073
uc3 = 0.021
mean23 = c(mu2,mu3)
sigma3 = matrix(c(uc2^2,0.228*uc2*uc3,0.228*uc2*uc3,uc3^2), nrow = 2)
lower = rep(0,2)
upper = rep(100,2)

prior23 = rtmvnorm(n,mean23,sigma3,lower,upper)
prior2 = prior23[,1]
prior3 = prior23[,2]
prior1 = c(rep(100,n)) - prior2 - prior3
prior123 = cbind(prior1,prior2,prior3)
prior = prior123[prior123[,1]>=0,]  # Only generated vectors in which X values are non-negative
are retained
prior1 = prior[,1]
prior2 = prior[,2]
prior3 = prior[,3]

# Correlation matrix of the modelled multivariate prior PDF
cor(prior)

# Joint coverage probability
Pcov123 = length(prior[(prior1>=lrl1 & prior1<=url1) & (prior2>=lrl2 & prior2<=url2) &
(prior3>=lrl3 & prior3<=url3)])/(3*n)

# X Marginal coverage probability
Pcov1 = length(prior1[prior1>=lrl1 & prior1<=url1])/length(prior1)

# Y Marginal coverage probability
Pcov2 = length(prior2[prior2>=lrl2 & prior2<=url2])/length(prior1)

# Z Marginal coverage probability
Pcov3 = length(prior3[prior3>=lrl3 & prior3<=url3])/length(prior1)
```

```
############
# MODEL 3

n = 10000000
mu2 = 7.547
mu3 = 0.059
uc2 = 0.073
uc3 = 0.021

prior2 = rtnorm(n,mu2,uc2,0,100)
prior3 = rtnorm(n,mu3,uc3,0,100-prior2)
prior1 = c(rep(100,n)) - prior2 - prior3
prior = cbind(prior1,prior2,prior3)

# Correlation matrix of the modelled multivariate prior PDF
cor(prior)

# Joint coverage probability
Pcov123 = length(prior[(prior1>=lrl1 & prior1<=url1) & (prior2>=lrl2 & prior2<=url2) &
(prior3>=lrl3 & prior3<=url3)])/(3*n)

# X Marginal coverage probability
Pcov1 = length(prior1[prior1>=lrl1 & prior1<=url1])/n

# Y Marginal coverage probability
Pcov2 = length(prior2[prior2>=lrl2 & prior2<=url2])/n

# Z Marginal coverage probability
Pcov3 = length(prior3[prior3>=lrl3 & prior3<=url3])/n
```

B.2. Calculation of the total global risks

```
# Inizializations and setting
library(mvtnorm)
library(msm)
library(tmvtnorm)
library(compositions)
library(nortest)

rm(list=ls())

lrl1 = 92.2            # Lower regulation limit
url1 = 92.8            # Upper regulation limit
```

```
lrl2 = 7.3              # Lower regulation limit
url2 = 7.7              # Upper regulation limit
lrl3 = 0                # Lower regulation limit
url3 = 0.18             # Upper regulation limit
lal1 = lrl1             # Lower acceptance limit
lal2 = lrl2             # Lower acceptance limit
lal3 = lrl3             # Lower acceptance limit
ual1 = url1             # Upper acceptance limit
ual2 = url2             # Upper acceptance limit
ual3 = url3             # Upper acceptance limit
lrl = c(lrl1,lrl2,lrl3)
url = c(url1,url2,url3)
lal = c(lal1,lal2,lal3)
ual = c(ual1,ual2,ual3)


mu1 = 92.483            # Prior mean value of the true results
mu2 = 7.457             # Prior mean value of the true results
mu3 = 0.059             # Prior mean value of the true results
uc1 = 0.081             # Prior sd
uc2 = 0.073             # Prior sd
uc3 = 0.021             # Prior sd


rucm2 = 0.04/mu2*100        # RELATIVE (%) measurement uncertainty
rucm3 = 0.18*100           # RELATIVE (%) measurement uncertainty
rucm1 = sqrt(0.04^2+0.18^2*mu3^2+2*0.228*0.04*0.18*mu3)/mu1*100 #   RELATIVE   (%)
measurement uncertainty
ucm1 = rucm1*mu1/100       # ABSOLUTE (%) measurement uncertainty
ucm2 = rucm2*mu2/100       # ABSOLUTE (%) measurement uncertainty
ucm3 = rucm3*mu3/100       # ABSOLUTE (%) measurement uncertainty


############
# Model 1
mu = c(mu1,mu2,mu3)
sigma = matrix(c(uc1^2, -0.967*uc1*uc2, -0.467*uc1*uc3, -0.967*uc1*uc2, uc2^2,
0.228*uc2*uc3, -0.467*uc1*uc3, 0.228*uc2*uc3,uc3^2), nrow = 3)
sigma_lik = matrix(c(ucm1^2, -0.967*ucm1*ucm2, -0.467*ucm1*ucm3, -0.967*ucm1*ucm2,
ucm2^2, 0.228*ucm2*ucm3, -0.467*ucm1*ucm3, 0.228*ucm2*ucm3, ucm3^2), nrow = 3)


# PRIOR
n = 10000000
lowerT = rep(0,3)
upperT = rep(100,3)
prior = rtmvnorm(n,mu,sigma,lowerT,upperT)
prior = clo(prior, total = 100)


# LIKELIHOOD
```

```
like = prior + rtmvnorm(n, c(rep(0,3)), sigma_lik, lower = -mu, upper = 100 - mu)
like = clo(like, total = 100)

# PRODUCER'S RISK
m = 3 # Number of components
z=0
for(i in 1:n) {
if(all(prior[i,]>=lrl[1:m] & prior[i,]<=url[1:m]) & any(like[i,]>ual[1:m] | like[i,]<lal[1:m])) {
z=z+1}
}
RtotglobP = z/n

# CONSUMER'S RISK
m = 3 # Number of components
q=0
for(i in 1:n) {
if(all(like[i,]>=lal[1:m] & like[i,]<=ual[1:m]) & any(prior[i,]>url[1:m] | prior[i,]<lrl[1:m])) {
q=q+1}
}
RtotglobC = q/n


############
# Model 2
mu = c(mu2,mu3)
sigma = matrix(c(uc2^2, 0.228*uc2*uc3, 0.228*uc2*uc3, uc3^2), nrow = 2)
sigma_lik = matrix(c(ucm2^2, 0.228*ucm2*ucm3, 0.228*ucm2*ucm3, ucm3^2), nrow = 2)
lowerT = rep(0,2)
upperT = rep(100,2)

# PRIOR
n = 10000000
prior = rtmvnorm(n,mu,sigma,lowerT,upperT)
prior2 = prior[,1]
prior3 = prior[,2]
prior1 = c(rep(100,n)) - prior2 - prior3
prior123 = cbind(prior1,prior2,prior3)
prior = prior123[prior123[,1]>=0,]     # Only generated vectors in which X values are non-negative
are retained

# LIKELIHOOD
like23 = prior[,2:3] + rtmvnorm(n, c(rep(0,2)), sigma_lik, lower = -mu, upper = 100 - mu)
like2 = like23[,1]
like3 = like23[,2]
like1 = 100 - like2 - like3
like123 = cbind(like1,like2,like3)
```

```
like = like123[like123[,1]>=0,]
prior = prior[like123[,1]>=0,]        # Updated prior, disregarding values corresponding to
negative likelihood values for the first quantity

# PRODUCER'S RISK
m = 3 # Number of components
z=0
for(i in 1:dim(prior)[1]) {
if(all(prior[i,]>=lrl[1:m] & prior[i,]<=url[1:m]) & any(like[i,]>ual[1:m] | like[i,]<lal[1:m])) {
z=z+1}
}
RtotglobP = z/n

# CONSUMER'S RISK
m = 3 # Number of components
q=0
for(i in 1:dim(prior)[1]) {
if(all(like[i,]>=lal[1:m] & like[i,]<=ual[1:m]) & any(prior[i,]>url[1:m] | prior[i,]<lrl[1:m])) {
q=q+1}
}
RtotglobC = q/n


###########
# Model 3
n = 10000000
prior2 = rtnorm(n,mu2,uc2,0,100)
like2 = prior2 + rtnorm(n, 0, ucm2, lower = -prior2, upper = 100 - prior2)
prior3 = rtnorm(n,mu3,uc3,0,100-prior2)
like3 = prior3 + rtnorm(n, 0, ucm3, lower = -prior3, upper = 100 - like2 - prior3)
prior1 = c(rep(100,n)) - prior2 - prior3
like1 = 100 - like2 - like3
joint123 = cbind(prior1,prior2,prior3,like1,like2,like3)

# PRODUCER'S RISK
RtotglobP = length(joint123[(prior1>=lrl1 & prior1<=url1) & (prior2>=lrl2 & prior2<=url2) &
(prior3>=lrl3 & prior3<=url3) & (like1<lal1 | like1>ual1 | like2<lal2 | like2>ual2 | like3<lal3 |
like3>ual3)])/(6*n)

# CONSUMER'S RISK
RtotglobC = length(joint123[(like1>=lal1 & like1<=ual1) & (like2>=lal2 & like2<=ual2) &
(like3>=lal3 & like3<=ual3) & (prior1<lrl1 | prior1>url1 | prior2<lrl2 | prior2>url2 | prior3<lrl3 |
prior3>url3)])/(6*n)
```

References

[1] J.R. Dean, Extraction techniques in analytical science, Willey, Padstow, 2009.

[2] J. Dubrovkin, Mathematical processing of spectral data in analytical chemistry: A guide to error analysis, Cambridge Scholars Publishing, Cambridge, 2018.

[3] É.M.D.M. Flores (Ed.), Microwave-assisted sample preparation for trace element determination, Elsevier, Amsterdam, 2014.

[4] Bo E.H. Saxberg, B.R. Kowalski, Generalized standard additions method, Anal Chem 51 (1979) 1031-1038. https://doi.org/10.1021/ac50043a059.

[5] J. Vessman, R.I. Stefan, J.F. van Staden, K. Danzer, W. Lindner, D.T. Burns, A. Fajgelj and H. Müller, Selectivity in analytical chemistry (IUPAC Recommendations 2001), Pure and Appl Chem 73 (2001) 1381–1386. https://doi.org/10.1351/pac200173081381.

[6] B. Magnusson and U. Ornemark (Eds.), Eurachem Guide: The fitness for purpose of analytical methods – A laboratory guide to method validation and related topics. https://www.eurachem.org/index.php/publications/guides, 2014 (accessed 1 November 2019).

[7] JCGM 200, International Vocabulary of Metrology – Basic and General Concepts and Associated Terms. http://www.bipm.org/en/publications/guides/, 2012 (accessed 5 November 2019).

[8] ICH Harmonized Tripartite Guideline Q2(R1), Validation of analytical procedures: Text and methodology. https://www.ich.org/page/quality-guidelines, 2005 (accessed 1 November 2019).

[9] I. Kuselman and F. Pennecchi, IUPAC/CITAC Guide: Classification, modelling and quantification of human errors in chemical analytical laboratory (IUPAC Technical Report), Pure Appl Chem 88 (2016) 477-515. https://doi.org/10.1515/pac-2015-1101.

[10] F. Sherman and I. Kuselman, Stoichiometry and chemical metrology: Karl Fischer reaction, Accred Qual Assur 4 (1999) 230-234. https://doi.org/10.1007/s007690050357.

[11] K. Schwahn, R. Beleggia, N. Omranian and Z. Nikoloski, 2017. Stoichiometric correlation analysis: Principles of metabolic functionality from metabolomics data. Front Plant Sci. 8, 2152. https://doi.org/10.3389/fpls.2017.02152.

[12] L. Wang, P. Wang, M. Sheng and J. Tian, 2018. Ecological stoichiometry and environmental influencing factors of soil nutrients in the karst rocky desertification ecosystem, southwest China. Global Ecology and Conservation. 16, e00449. https://doi.org/10.1016/j.gecco.2018.e00449.

[13] I. Kuselman, F.R. Pennecchi, R.J.N.B. da Silva, D.B. Hibbert, Risk of false decision on conformity of a multicomponent material when test results of the components' content are correlated, Talanta 174 (2017) 789-796. https://doi.org/10.1016/j.talanta.2017.06.073.

[14] I. Kuselman, F.R. Pennecchi, R.J.N.B. da Silva, D.B. Hibbert, E. Anchutina, Total risk of false decision on conformity of an alloy due to measurement uncertainty and correlation of test results, Talanta 189 (2018) 666-674. https://doi.org/10.1016/j.talanta.2018.07.049.

[15] F. Chayes, On correlation between variables of constant sum, J Geophys Res 65 (1960) 4185-4193. https://doi.org/10.1029/JZ065i012p04185.

[16] T. Vigen, Spurious correlations, Hachette Books, New York – Boston, 2015.

[17] P. Kynčlová, K. Hron, P. Filmoser, Correlation between compositional parts based on symmetric balances, Math Geosci 49 (2017) 777-796. https://doi.org/10.1007/s11004-016-9669-3.

[18] J. Aitchison, The statistical analysis of compositional data, Chapman and Hall, London, 1986.

[19] J. Aitchison, Principles of compositional data analysis, in: T.W. Anderson, K.T. Fang and I. Olkin (Eds.), Multivariate Analysis and its Applications, IMS Lecture Notes – Monograph Series, Hayward, CA: Institute of Mathematical Statistics, Vol. 24, 1994, pp. 73-81. https://doi.org/10.1214/lnms/1215463786.

[20] J. Aitchison, A concise guide to compositional data analysis, ebook. https://www.goodreads.com/book/show/46756704-a-concise-guide-to-compositional-data-analysis, 2003 (accessed 1 November 2019).

[21] V. Pawlowsky-Glahn, A. Buccianti, Compositional data analysis: theory and applications, Wiley, Chichester, 2011.

[22] M. Greenacre, E.C. Grunsky, 2018. The isometric logratio transformation in compositional data analysis: A practical evaluation. ResearchGate. http://doi.org/10.13140/RG.2.2.10817.20322.

[23] M. Greenacre. Variable selection in compositional data analysis using pairwise logratios, Math Geosci 51 (2019) 649-682. https://doi.org/10.1007/s11004-018-9754-x.

[24] M. Greenacre. Compositional data analysis in practice, CRC Press, Boca Raton, 2019.

[25] A. Buccianti, Is compositional data analysis a way to see beyond the illusion? Comput Geosci 50 (2013) 165-173. http://dx.doi.org/10.1016/j.cageo.2012.06.012.

[26] A. Buccianti, E. Grunsky, Compositional data analysis in geochemistry: Are we sure to see what really occurs during natural processes? J Geochem Explor 141 (2014) 1-5. http://dx.doi.org/10.1016/j.gexplo.2014.03.022.

[27] P. Filzmoser, K. Hron, C. Reimann, The bivariate statistical analysis of environmental (compositional) data, 408 (2010) 4230-4238. https://doi.org/10.1016/j.scitotenv.2010.05.011.

[28] C. Reimann, P. Filzmoser, K. Fabian, M. Birke, A. Demetriades, E. Dinelli, A. Ladenberger and the GEMAS Project Team, The concept of compositional data analysis in practice – Total major element concentrations in agricultural and grazing land soils of Europe, Sci Total Environ 426 (2012) 196-210. https://doi.org/10.1016/j.scitotenv.2012.02.032.

[29] M.E. Edjabou, J.A. Martin-Fernandez, C. Scheutz, T.F. Astrup, Statistical analysis of solid waste compositional data: Arithmetic mean, standard deviation and correlation coefficients, Waste Manage 69 (2017) 13-23. http://dx.doi.org/10.1016/j.wasman.2017.08.036.

[30] H.A. Souza, S.E. Parent, D.E. Rozane, D.A. Amorim, V.C.Modesto, W. Natale, L.E. Parent, Guava waste to sustain guava (Psidium guajava) agroecosystem: Nutrient "balance" concepts. Front Plant Sci. 7, 1252. https://doi.org/10.3389/fpls.2016.01252.

[31] J.M. Macklaim, G.B. Gloor, From RNA-seq to biological inference: Using compositional data analysis in meta-transcriptomics, in: R. Beiko, W. Hsiao, J. Parkinson (Eds.), Microbiome analysis. Methods in molecular biology, Vol. 1849, Humana Press, New York, 2018, pp. 193-213.

[32] T.P. Quinn, I. Erb, M.F. Richardson, T.M. Crowley, Understanding sequencing data as compositions: an outlook and review, Bioinformatics 34 (2018) 2870-2878. https://doi.org/10.1093/bioinformatics/bty175.

[33] G.P. Campbell, J.M. Curran, G.M. Miskelly, S. Coulson, G.M. Yaxley, E.C. Grunsky, S.C. Cox, Compositional data analysis for elemental data in forensic science, Forensic Sci Int 188 (2009) 81-90. https://doi.org/10.1016/j.forsciint.2009.03.018.

[34] T. Neocleous, C. Aitken, G. Zadora, Transformations for compositional data with zeros with an application to forensic evidence evaluation, Chemometr Itell Lab Syst 109 (2011) 77-85. https://doi.org/10.1016/j.chemolab.2011.08.003.

[35] M.Z. Peterson, S.K. Suram, J.M. Gregoire. Statistical analysis and interpolation of compositional data in materials science, ACS Comb Sci 17 (2015) 130-136. https://doi.org/10.1021/co5001458.

[36] Compositional Data Analysis Website (CODAWEB). http://www.compositionaldata.com/, 2019 (accessed 1 November 2019).

[37] J. Aitchison, The single principle of compositional data analysis, continuing fallacies, confusions and misunderstandings and some suggested remedies, in: J. Daunis-i-Estadella, J.A. Martín-Fernández (Eds.), Proceedings of CODAWORK'08, The 3rd Compositional Data Analysis Workshop, University of Girona, 2008, CD-ROM, ISBN: 978-84-8458-272-4. https://dugi-doc.udg.edu//handle/10256/706 (accessed 1 November 2019).

[38] A.M.H. van der Veen, K. Hafner, Atomic weights in gas analysis, Metrologia 51 (2014) 80-86. https://doi.org/10.1088/0026-1394/51/1/80.

[39] M.J.T. Milton, G.M. Vargha, A.S. Brown, Gravimetric methods for preparation of standard gas mixtures, Metrologia 48 (2011) R1-R9. https://goi.org/10.1088/0026-1394/48/5/R01.

[40] ISO Guide 35, Reference materials – Guidance for characterization and assessment of homogeneity and stability, ISO, Geneva, 2017.

[41] S. Westwood, T. Choteau, A. Daireaux, R.D. Josephs, R.I. Wiegosz, mass balance method for the SI value assignment of the purity of organic compounds, ACS Anal Chem 85 (2013) 3118-3126. http://dx.doi.org/10.1021/ac303329k.

[42] S.R. Davies, M. Alamgir, B.K.H. Chan, T. Dang, K. Jones, M. Krishnaswami, Y. Luo, P.S.R. Mitchell, M. Moawad, H. Swan, G.J. Tarrant, The development of an efficient mass balance approach for the purity assignment of organic calibration standards, Anal Bioanal Chem 407 (2015) 7983-7993. https://doi.org/10.1007/s00216-015-8971-0.

[43] A.C.P. Osorio, R.C. de Sena, T.O. Araújo, M.D. de Almeida, Purity assessment using the mass balance approach for inorganic in-house certified reference material production at Inmetro, Accred Qual Assur 24 (2019) 387-394. https://doi.org/10.1007/s00769-019-01392-w.

[44] I. Kuselman, F.R. Pennecchi, R.J.N.B. da Silva, D.B. Hibbert, Conformity assessment of multicomponent materials or objects: Risk of false decisions due to measurement uncertainty – A case study of denatured alcohols, Talanta 164 (2017) 189-195. http://dx.doi.org/10.1016/j.talanta.2016.11.035.

[45] F.R. Pennecchi, I. Kuselman, R.J.N.B. da Silva, D.B. Hibbert, Risk of false decision on conformity of an environmental compartment due to measurement uncertainty of concentrations of two or more pollutants, Chemosphere 202 (2018) 165-176. https://doi.org/10.1016/j.chemosphere.2018.03.054.

[46] R.J.N.B. da Silva, F.R. Pennecchi, D.B. Hibbert, I. Kuselman, Tutorial and spreadsheets for Bayesian evaluation of risks of false decisions on conformity of a multicomponent material or object due to measurement uncertainty, Chemometr Intell Lab Syst 182 (2018) 109-116. https://doi.org/10.1016/j.chemolab.2018.09.004.

[47] R.J.N.B. da Silva, F.R. Lourenço, F.R. Pennecchi, D.B. Hibbert, I. Kuselman, Spreadsheet for evaluation of global risks in conformity assessment of a multicomponent material or object, Chemometr Intell Lab Syst 188 (2019) 1-5. https://doi.org/10.1016/j.chemolab.2019.02.010.

[48] IUPAC Project 2019-012-1-500, Influence of a mass balance constraint on uncertainty of test results of a substance or material and risks in its conformity assessment, 2019. https://iupac.org/project/2019-012-1-500.

[49] JCGM 106, Evaluation of Measurement Data – The Role of Measurement Uncertainty in Conformity Assessment. http://www.bipm.org/en/publications/guides/, 2012 (assessed 17 December 2019)

[50] I. Kuselman, F. Pennecchi, C. Burns, A. Fajgelj, P. de Zorzi, IUPAC/CITAC Guide: Investigating out-of-specification test results of chemical composition based on metrological concepts (IUPAC Technical Report), Pure Appl Chem 84 (2012) 1939-1971. https://doi.org/10.1351/PAC-REP-11-10-04.

[51] JCGM 101, Evaluation of measurement data — Supplement 1 to the "Guide to the expression of uncertainty in measurement" — Propagation of distributions using a Monte Carlo method. http://www.bipm.org/en/publications/guides/, 2008, Clauses 6.4.7-6.4.8 (assessed 17 December 2019).

[52] A. Taavitsainen, R. Vanhanen, On the maximum entropy distributions of inherently positive nuclear data, Nucl Instrum Methods Phys Res A854 (2017) 156-162. http://dx.doi.org/10.1016/j.nima.2016.11.061.

[53] F. Cosman, E. Krotkov, Truncated Gaussians as Tolerance Sets, CMU-RI-TR 94-35, Carnegie Mellon University,

https://www.ri.cmu.edu/pub_files/pub1/cozman_fabio_1994_1/cozman_fabio_1994_1.pdf, 1994 (assessed 17 December 2019).

[54] X. Dong, Whisker of boxplot, R-bloggers, https://www.r-bloggers.com/whisker-of-boxplot/, 2012 (assessed 7 January 2020).

[55] JCGM 100, Evaluation of measurement data – Guide to the expression of uncertainty in measurement. http://www.bipm.org/en/publications/guides/, 2008, Clause 5.2.2 (assessed 11 January 2020).

[56] I. Kuselman, F.R. Pennecchi, R.J.N.B. da Silva, D.B. Hibbert, How many shades of grey are in conformity assessment due to measurement uncertainty? J Phys: Conf Series 1420 (2019) 012001. https://doi.org/10.1088/1742-6596/1420/1/012001.

[57] S. Wilhelm, RDocumentation, rtmvnorm, Sampling random numbers from the truncated multivariate normal distribution. https://www.rdocumentation.org/packages/tmvtnorm/versions/1.4-10/topics/rtmvnorm (assessed 29 January 2020).

[58] J. Hadfield. RDocumentation, rtnorm, Random generation from a truncated normal distribution. https://www.rdocumentation.org/packages/MCMCglmm/versions/2.29/topics/rtnorm (assessed 29 January 2020).

[59] K. G. van den Boogaart, R. Tolosana-Delgado, M. Bren, Compositional data analysis. https://cran.r-project.org/web/packages/compositions/compositions.pdf, 2019 (assessed 25 January 2020)

Figure captions

Fig. 1. Metrologically-related correlation arising in a multicomponent chemical analysis - the Swiss-cheese model.

Fig. 2. Orthogonal coordinates (Euclidian space) and simplex. The variables c_i are contents of material components i = 1, 2, 3 and 4, %; each simplex vertex is c_i = 100 %; D is dimension. In each case mass balance constraint reduces the number of dimensions by one.

Fig. 3. Boxplots of the marginal prior pdfs of the components' contents. Boxplot 1 is before closure operation, and boxplot 2 after it; for a) Pt content, c_1; b) Rh content, c_2; and c) content of the eight impurities, c_3. The band near the middle of each box is the 50 % percentile (the median, equal to the mean when the distribution is symmetrical); the bottom and top of the box corresponds to 25 % and 75 % percentiles, respectively; the distance between upper and/or lower whiskers and the box is equal to the 1.5 box length [54].

Fig. 4. Histogram of the marginal pdf of the Pt content, c_1. Pink bars show frequencies of the Pt content (fractions of 1×10^7 MC simulations) before the closure operation, while blue bars present the frequencies after this operation (i.e. after taking into account the mass balance constraint).

Fig. 5. **Surfaces of the total global consumer's risk R_c and producer's risk R_p vs. acceptance intervals for measured Rh content (A_2) and measured content of the eight impurities (A_3).** The arrows show the acceptance intervals from $A_2 = T_2$ and $A_3 = T_3$ at the axes beginning, to the acceptance intervals with limits differing from the tolerance limits by three times the relevant measurement uncertainties at the axes end, when for Pt content $A_1 = T_1$. The color column bar in plot 5a gives indication of the R_c values between the minimum and the maximum on the surface, i.e. from 3×10^{-6} to 4.7×10^{-3}; in plot 5b the bar is for the R_p values between 4.9×10^{-3} and 2.4×10^{-2}.

Fig. 1

Metrologically-related correlation

1) **Development of the method (digestion, extraction, separation, chemometrics processing spectral data, st. additions, etc.)**

2) **Validation of SOP (analytical selectivity, specificity)**

3) **Training analysts and proficiency testing**

4) **Supervision & quality control**

Quality system of a lab

Correlated test results

Fig. 2

c_1

c_2

2D → 1D

c_1 ——— c_2

$c_1 + c_2 = 100\ \%$

c_1

c_3

c_2

3D → 2D

c_3
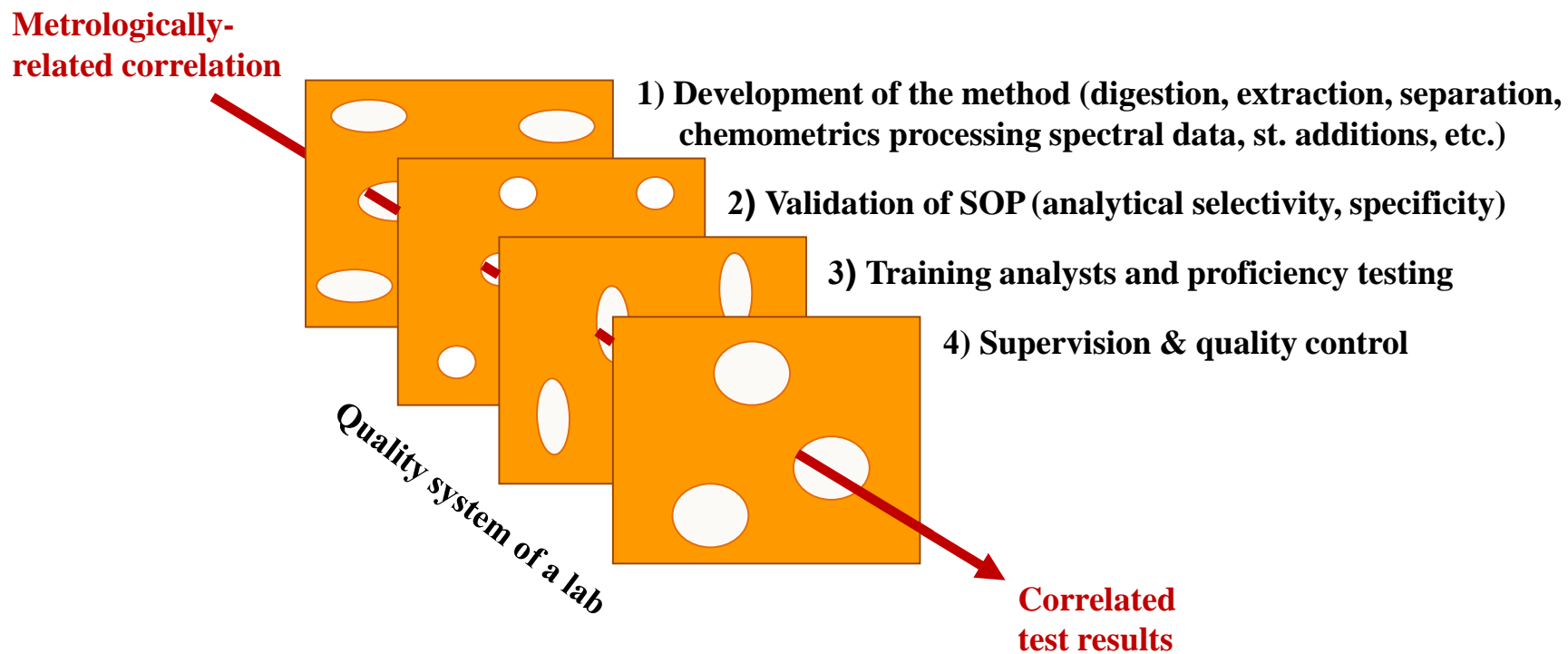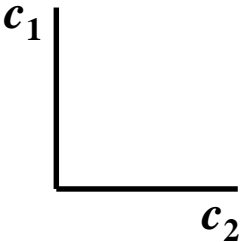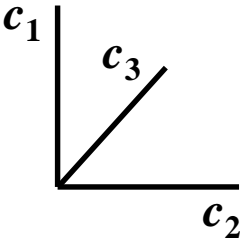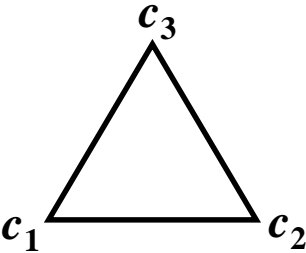
c_1 c_2

$c_1 + c_2 + c_3 = 100\ \%$

Orthogonal/Euclidian 4D → 3D

c_4

c_3
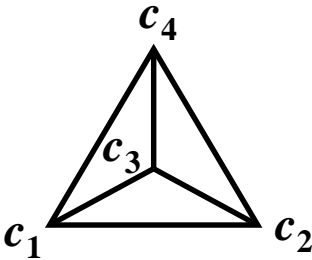
c_1 c_2

$c_1 + c_2 + c_3 + c_4 = 100\ \%$

Fig. 3

Fig. 4

Fraction of $1 \cdot 10^7$

c_1 (% mass)
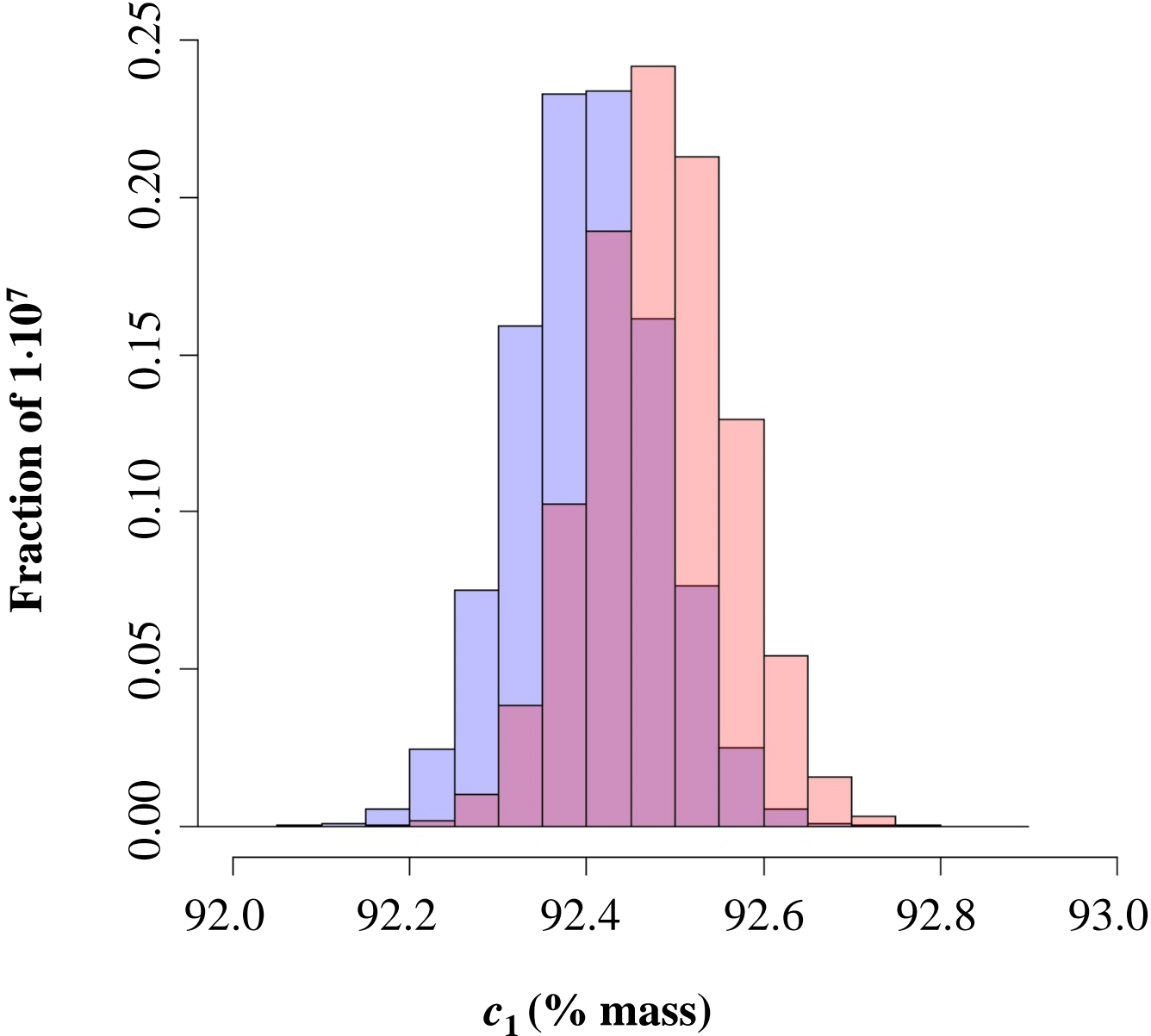
Fig. 5
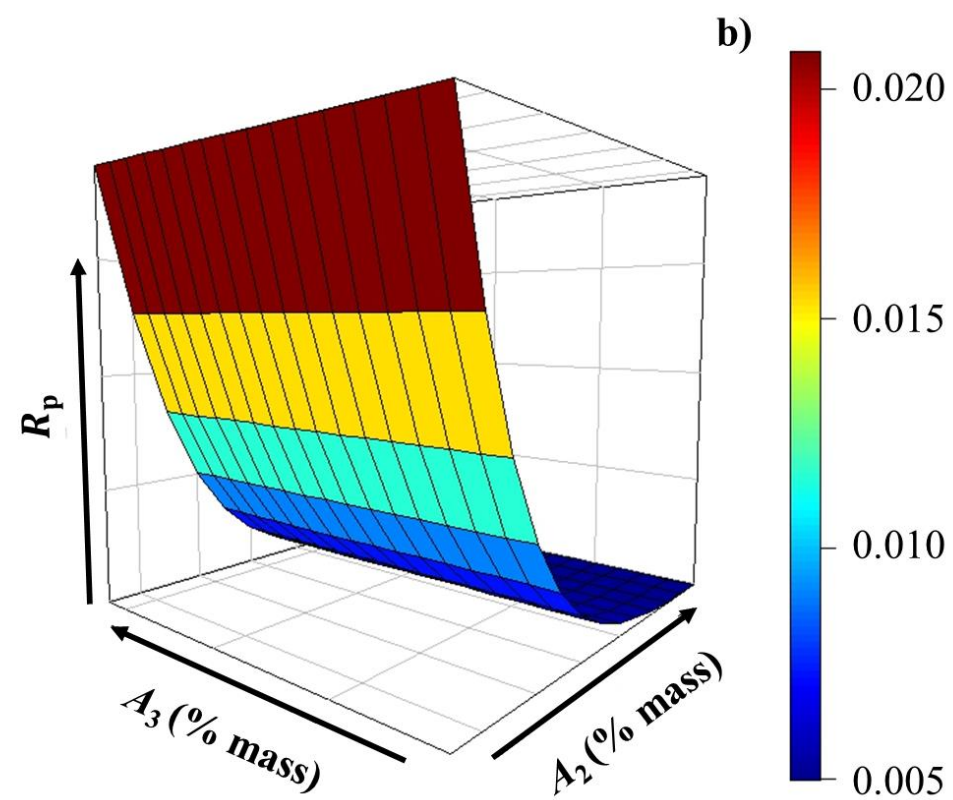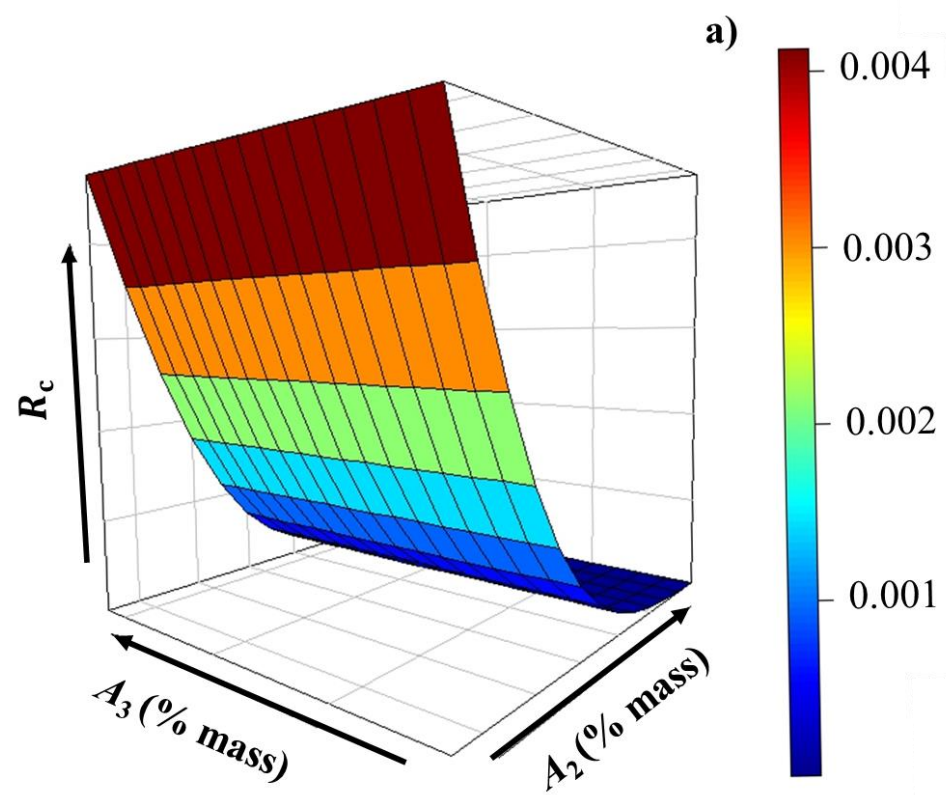
Table 1. Parameters of the prior distribution and measurement uncertainties for a PtRh alloy [14].

component	i	μ_i , %	σ_i, %	ij	r_{ij}
Pt	1	92.483	0.081	12	-0.967
Rh	2	7.457	0.073	13	-0.467
8 impurities	3	0.059	0.021	23	0.228

Table 2. Correlation coefficients and coverage probabilities calculated from 10^7 Monte Carlo simulations for the PtRh alloy system

Parameters	Model		
	1	2	3
r_{12}	-0.968	-0.968	-0.962
r_{13}	-0.464	-0.464	-0.274
r_{23}	0.226	0.226	0.000
p	0.985	0.981	0.981

Declaration of interests

☒ The authors declare that they have no known competing financial interests or personal relationships that could have appeared to influence the work reported in this paper.

☐The authors declare the following financial interests/personal relationships which may be considered as potential competing interests: